

RAPID COSMIC-RAY ACCELERATION AT PERPENDICULAR SHOCKS IN SUPERNOVA REMNANTS

MAKOTO TAKAMOTO^{1,2} AND JOHN G. KIRK¹

¹Max-Planck-Institut für Kernphysik, Postfach 103980, 69029 Heidelberg, Germany

²Department of Earth and Planetary Science, The University of Tokyo, 7-3-1 Hongo, Bunkyo-ku, Tokyo 113-0033, Japan

Draft version December 20, 2021

ABSTRACT

Perpendicular shocks are shown to be rapid particle accelerators that perform optimally when the ratio u_s of the shock speed to the particle speed roughly equals the ratio $1/\eta$ of the scattering rate to the gyro frequency. We use analytical methods and Monte-Carlo simulations to solve the kinetic equation that governs the anisotropy generated at these shocks, and find, for $\eta u_s \approx 1$, that the spectral index softens by unity and the acceleration time increases by a factor of two compared to the standard result of diffusive shock acceleration theory. These results provide a theoretical basis for the thirty-year-old conjecture that a supernova exploding into the wind of a Wolf-Rayet star may accelerate protons to an energy exceeding 10^{15} eV.

Subject headings: acceleration of particles — cosmic rays — shock waves — supernovae: general

1. INTRODUCTION

The “knee” at $\sim 5 \times 10^{15}$ eV in the energy spectrum of cosmic rays arriving at Earth defines a characteristic energy that can be used to constrain the physics of the acceleration and propagation of these particles. Ideally, a theory of cosmic-ray acceleration would provide a natural explanation of this feature. Diffusive shock acceleration (DSA) in supernova remnants (SNR), together with the associated amplification of the ambient magnetic field, is in many respects a convincing theory, but it fails to deliver a simple prediction of the energy of the knee. The maximum energy to which it can operate lies somewhat below 10^{15} eV, and is thought to be governed by the level at which the nonlinear process of magnetic field amplification saturates. It is not known how higher energy particles could be produced by within this theory (for a recent review, see Bell 2014).

The basic problem was identified long ago (Lagage & Cesarsky 1983a,b; Hillas 2005): DSA is too slow, because particles that cross and recross a shock front are accelerated at a rate t_{acc}^{-1} , that is second order in the small parameter $\epsilon = u_s/v$: $t_{\text{acc}}^{-1} \sim \epsilon^2 \omega_g$, where u_s is the shock velocity, v the particle speed, and $\omega_g = Ze|Bc/E$ is the (angular) gyro-frequency of a cosmic ray of charge Ze and energy E in a magnetic field B . Given this timescale, the only way for a SNR to accelerate particles up to the knee is by generating a magnetic field at the shock front that is substantially stronger than that in the surrounding medium. Magnetic field amplification in SNR is consistent with the observation of thin X-ray filaments in SNR (Völk et al. 2005; Parizot et al. 2006), and emerges from numerical simulations of parallel shocks using both particle-in-cell and hybrid codes (Reville & Bell 2012; Matsumoto et al. 2013; Caprioli & Spitkovsky 2014; Matsumoto et al. 2015). However, it appears to saturate at a level that does not permit acceleration to energies above the knee (Bell et al. 2013).

In a seminal paper, Jokipii (1987) (see also Ostrowski

(1988)) noted that this problem is characteristic of parallel shocks, at which particles cross and recross the shock by diffusing along field lines, which leads to a relatively long cycle time compared to the gyro period, particularly if the scattering rate is low. At a perpendicular shock, on the other hand, the cycle time is close to the gyro period. If DSA were to remain valid, this would give an acceleration rate $t_{\text{acc}}^{-1} \sim \epsilon \omega_g$, which is fast enough to achieve energies well above the knee (Biermann 1993). The existence of a characteristic energy at 5×10^{15} eV could then plausibly be associated with a change in the confinement properties of the SNR (Drury 2011; Malkov et al. 2013), since the gyro radius of a proton of this energy in the interstellar magnetic field is comparable with the radius of a SNR entering its Sedov phase of expansion.

Early attempts to resolve this question using a Monte-Carlo approach for nonrelativistic shocks were forced to make strong simplifications. Baring et al. (1993), for example, used a guiding center approximation that implicitly assumes the distribution is almost independent of gyro-phase. In later work (Ellison et al. 1995) this was lifted, and agreement with the predictions of DSA over a limited range of shock obliquities was found. However, a large-angle scattering algorithm was used that strongly affects the ability to resolve anisotropies at the shock. Takahara & Terasawa (1991) presented a method that takes full account of anisotropy and non-conservation of the first adiabatic invariant (magnetic moment), but neglected the transport of particles across field lines — a crucial ingredient for the treatment of perpendicular shocks. Meli & Biermann (2006) investigated both the spectrum and acceleration timescale for highly oblique shocks, and found that both quantities agreed with the DSA predictions even for low scattering rates. However, they also used a guiding center approach, which can be justified only if the scattering rate is high.

Later work has lifted these artificial restrictions, although the regime of nonrelativistic shock speeds and low scattering rates remains challenging. The softening of the accelerated particle spectrum at a perpendicular shocks of speed above $u_s = 0.1c$ was investigated quantitatively

by Summerlin & Baring (2012), who used Monte-Carlo simulations. Using a finite-difference method to solve the equations that result from an expansion of the distribution function in spherical harmonics, Bell et al. (2013) also noted this effect for perpendicular shocks of speed above $u_s = 0.03c$. In both cases, the results are in qualitative agreement with those presented below.

An alternative approach, pioneered by Decker & Vlahos (1986) and pursued, for example, by Ostrowski (1993) and Giacalone & Jokipii (1996) consists of specifying the turbulent field around a shock front explicitly, and examining the statistical properties of a large number of trajectories computed by numerically integrating the equations of motion. Evidence of an enhanced acceleration rate at oblique and perpendicular shocks was indeed found using this technique. Its advantages are that it allows insight to be gained at the microscopic level by studying individual trajectories, and has the potential to include the effects of anomalous transport (le Roux et al. 2010), which are not easily accessible in a Monte-Carlo approach.

Our main goal here is a quantitative resolution of these issues. We adopt a plausible microscopic model of the scattering process and solve for the full angular dependence of the distribution function, using both a Monte-Carlo approach and an analytic approximation obtained in the limit of small shock speed and low scattering rate. Our main results consist of the spectral index and the acceleration rate as functions of the shock speed, and the scattering rate.

In Section 2 we introduce the idealized model that is used to describe particle transport, and, in this context, discuss DSA at oblique and perpendicular shocks in more detail. The analytic approximation is presented in Section 3 and the Monte-Carlo method described in Section 4. The main results are presented in Section 5, and their implications for the acceleration of cosmic rays are discussed in Section 6. Section 7 summarizes our conclusions.

2. THE TRANSPORT MODEL

We consider the idealized situation of a plane shock front propagating at constant speed into a uniformly magnetized plasma. Cosmic rays are energetic charged particles, whose gyro radius is assumed to be large compared to the thickness of the shock front, which can, therefore, be treated as a discontinuity in the plasma velocity. The assumptions of constant, uniform fluid velocity and magnetic field are justified because we concentrate on the highest energy particles, whose energy density is much smaller than that of the bulk of the cosmic rays, which, in turn, is at most comparable to the ram pressure of the plasma flowing into the shock.

In general, the cosmic-ray distribution function $f(t, \vec{x}, \vec{p})$ is a function of time t , position \vec{x} and momentum \vec{p} . It is usual to assume that particles are continually deflected by magnetic fluctuations whose effect can be modeled as isotropic diffusion in the direction of motion, i.e., as diffusion on the sphere of the end-point of the unit vector \vec{p}/p , in addition to gyrating about the ambient magnetic field. This can be described by the Fokker-Planck equation, (e.g., Bell et al. 2011) which, in the case of a homogeneous magnetic field \vec{B} embedded

in a background plasma that is at rest, reduces to

$$\frac{\partial f}{\partial t} + \vec{v} \cdot \vec{\nabla} f + \omega_g \frac{\partial f}{\partial \phi} = \frac{\nu_{\text{coll}}}{2} \left[\frac{1}{\sin \theta} \frac{\partial}{\partial \theta} \left(\sin \theta \frac{\partial f}{\partial \theta} \right) + \frac{1}{\sin^2 \theta} \frac{\partial^2 f}{\partial \phi^2} \right], \quad (1)$$

where $\vec{v} = \vec{p}/E$ is the CR velocity, θ and ϕ are the spherical polar coordinates in momentum space with axis along \vec{B} , and ν_{coll} is a measure of the amplitude of the fluctuations, which is usually called the “collision frequency”. The assumption of *isotropic* diffusion in angle implies that ν_{coll} is independent of θ and ϕ . In the following, we consider a situation in which the shock front is a discontinuity that separates two half-spaces (upstream and downstream) in each of which equation (1) holds. Cosmic rays are assumed to cross this discontinuity without deflection, so that Liouville’s theorem can be used to relate the distribution immediately upstream (at $t = t_+$, $\vec{x} = \vec{x}_+$) to that immediately downstream (at $t = t_-$, $\vec{x} = \vec{x}_-$):

$$f(t_+, \vec{x}_+, \theta_+, \phi_+, p_+) = f(t_-, \vec{x}_-, \theta_-, \phi_-, p_-) \quad (2)$$

where p_{\pm} , θ_{\pm} , and ϕ_{\pm} are the upstream and downstream momentum coordinates that label the same momentum vector just as t_{\pm} and x_{\pm} label the same space-time point. These quantities are connected by a Lorentz boost, including, in general, a rotation to take account of the change in the direction of \vec{B} across the shock.

Equations (1) and (2) suffice to describe the particle acceleration process: solving the kinetic equation (1) in the presence of a moving boundary (the shock front) yields the particle residence times and escape probabilities, and connecting the upstream and downstream solutions using Liouville’s theorem (2) implements the boost in the energy measured in the local fluid frame which each particle experiences when it crosses the shock front. It is interesting to note that a very similar system was analyzed by Schatzman (1963), who, however, restricted the scattering to changes in phase, and considered only those particles whose trajectories are almost tangential to the shock. This limited the range of validity of the treatment to $\eta u_s \gg 1$ (in the notation used below), thereby delaying the discovery of DSA by fifteen years.

2.1. The diffusion approximation

If the cosmic ray distribution is almost isotropic, the angular dependence in equation (1) can be eliminated by expanding the momentum dependence of f in spherical harmonics (Jokipii 1971; Kingham & Bell 2004). DSA is based on solving the resulting spatial diffusion equation in the presence of a shock; a particularly useful introduction is given by Drury (1983), and this section reproduces the relevant results in order to facilitate the subsequent discussion. Many analytic solutions are available, of which two are of particular interest here. The first is for a steady-state particle distribution, with no cosmic rays far upstream and no source term above momentum p_0 . In this case, the distribution downstream does not depend on position, and is a power-law in momentum:

$$f(p) \propto H(p - p_0) p^{-s} \quad (3)$$

$$s = 3r / (r - 1) \quad (4)$$

where r is the compression ratio of the shock and $H(x)$ is the Heaviside (or “step”) function. Importantly, this solution is independent of \vec{B} , so that, within the diffusion approximation, shocks of all obliquities, including exactly parallel and perpendicular shocks, produce the same spectral index. The second solution gives the mean time $\langle t \rangle$ taken for a particle to be accelerated from momentum p_0 to momentum p_1 at an oblique shock (see Drury 1983, Eq 3.31):

$$\langle t \rangle = \frac{3}{u_+ - u_-} \int_{p_0}^{p_1} \frac{dp}{p} \left(\frac{\kappa_+}{u_+} + \frac{\kappa_-}{u_-} \right), \quad (5)$$

Here, u_+ (u_-) is the component of the plasma velocity upstream (downstream) along the shock normal, in a frame in which the shock is at rest and κ_{\pm} are the corresponding components of the diffusion tensor:

$$\kappa_{\pm} = \kappa_{\parallel\pm} \cos^2 \Psi_{\pm} + \kappa_{\perp\pm} \sin^2 \Psi_{\pm}, \quad (6)$$

with Ψ_{\pm} the angle between the magnetic field and the shock normal. In this notation, the shock velocity $u_s = u_+$ and the compression ratio $r = u_+/u_-$.

Applying the diffusion approximation to equation (1), Jokipii (1987) showed that the diffusion coefficients parallel and perpendicular to the magnetic field are related to the collision frequency by

$$\kappa_{\parallel} = \eta \frac{r_g v}{3}, \quad \kappa_{\perp} = \frac{\eta}{1 + \eta^2} \frac{r_g v}{3}, \quad (7)$$

where $r_g = v/\omega_g$ and the dimensionless parameter

$$\eta = \omega_g/\nu_{\text{coll}} \quad (8)$$

describes the degree to which the particles are magnetized.

If η is chosen to be a constant (independent not only of θ and ϕ , but also of p), eq (5), results in a mean acceleration rate proportional to p^{-1} . Discussions of DSA conventionally adopt this scaling together with the additional restriction $\eta_{\pm} \geq 1$. Although the applicability of these assumptions is disputed even within the framework of the diffusion approximation (Shalchi 2009; Ferrand et al. 2014), we nevertheless adopt them here, since our discussion focuses on the validity of the diffusion approximation itself.

The acceleration rate t_{acc}^{-1} for a relativistic particle, assuming, for simplicity, that η is the same in the upstream and downstream plasmas, and that $p \gg p_0$, is given by equation (5):

$$\begin{aligned} t_{\text{acc}}^{-1} &\equiv \langle t \rangle^{-1} \\ &= \omega_g \frac{u_+^2}{c^2} \frac{r-1}{\eta r} \left[\cos^2 \Psi_+ + \frac{\sin^2 \Psi_+}{1 + \eta^2} + \right. \\ &\quad \left. \frac{r B_+}{B_-} \left(\cos^2 \Psi_- + \frac{\sin^2 \Psi_-}{1 + \eta^2} \right) \right]^{-1}. \end{aligned} \quad (9)$$

At a parallel shock ($\Psi_{\pm} = 0$, $B_- = B_+$) equation (9), together with the restriction $\eta > 1$ gives an upper limit

on the acceleration rate:

$$\begin{aligned} t_{\text{acc}}^{-1} &< t_B^{-1} \\ &= \omega_g \frac{u_-^2}{c^2} \frac{r-1}{r(r+1)} \\ &\sim \mathcal{O}(\epsilon^2) \omega_g \end{aligned} \quad (10)$$

commonly referred to as the *Bohm limit*. On the other hand, at a perpendicular shock ($\Psi_{\pm} = \pi/2$, $B_- = r B_+$)

$$t_{\text{acc}}^{-1} = t_B^{-1} \frac{1 + \eta^2}{\eta} \frac{1 + r}{2} \quad (11)$$

and the acceleration rate rises linearly with η when $\eta \gg 1$ (Jokipii 1987). This behavior applies for all shocks with $\cos \Phi_- \lesssim 1/\eta$, which are sometimes called *quasi-perpendicular*, but, for simplicity, we restrict ourselves in the following to exactly perpendicular shocks.

3. APPROXIMATE ANALYTIC SOLUTIONS

Using “mixed” coordinates, in which \vec{p} (and \vec{v} , now expressed in units of c) are measured in the fluid rest frame, but \vec{x} and t are coordinates in a frame in which the shock is at rest, the transport equation (1) becomes:

$$\begin{aligned} (1 - v_z u) \frac{\partial f}{\partial t} + (v_z - u) c \frac{\partial f}{\partial z} = \\ \frac{\omega_g}{\Gamma} \left\{ -\frac{\partial f}{\partial \phi} + \frac{1}{2\eta} \left[\frac{\partial}{\partial \mu} (1 - \mu^2) \frac{\partial f}{\partial \mu} + \frac{1}{1 - \mu^2} \frac{\partial^2 f}{\partial \phi^2} \right] \right\} \end{aligned} \quad (12)$$

Here, the shock normal is along the z -axis, and we express both the component v_z of the particle speed in this direction (measured in the fluid rest frame) as well as the speed u of the fluid (assumed to be directed along the shock normal) in units of c . The flow Lorentz factor is $\Gamma = 1/\sqrt{1 - u^2}$, and spatial variations in the plane of the shock are ignored, i.e., $\partial f/\partial x = \partial f/\partial y = 0$. The magnetic field is in the y - z plane, and $\mu = \cos \theta$, so that $v_z = v \sin \theta \sin \phi$ is a function of μ and ϕ . For cosmic rays, the particle velocity, v , is close to unity. Note that equation (12) is valid only for perpendicular shocks; the corresponding equation for subluminal shocks is given by Kirk & Heavens (1989).

Solutions that are stationary in the shock rest frame can be found by separating the variables in either the upstream or the downstream region:

$$f(z, \vec{p}) = F(p) \sum_i a_i e^{\Lambda_i z \omega_g / \Gamma c} Q_i(\mu, \phi) \quad (13)$$

where F is an arbitrary function of p , and the eigenvalues Λ_i and eigenfunctions Q_i obey

$$\begin{aligned} \Lambda_i (v_z - u) Q_i = \\ \left\{ -\frac{\partial}{\partial \phi} + \frac{1}{2\eta} \left[\frac{\partial}{\partial \mu} (1 - \mu^2) \frac{\partial}{\partial \mu} + \frac{1}{1 - \mu^2} \frac{\partial^2}{\partial \phi^2} \right] \right\} Q_i \end{aligned} \quad (14)$$

together with boundary conditions on Q_i that ensure regularity and single-valuedness on the sphere. In general, equation (14) has an infinite number of both positive and negative discrete eigenvalues (labeled with $i > 0$ and $i < 0$ respectively), in addition to the eigenvalue $\Lambda_0 = 0$

with eigenfunction $Q_0 = \text{constant}$. These govern the spatial dependence of the solution: the isotropic part is independent of z , whereas the eigenfunctions with $i < 0$ decay exponentially towards positive z (i.e., upstream), and grow exponentially downstream on a length scale that decreases as $|i|$ increases. Following the procedure used for relativistic shocks (Kirk & Schneider 1987) the solutions in the upstream and downstream regions can be matched at the shock to find the function $F(p)$, which, in the absence of a source term, is a scale-free power law $F \propto p^{-s}$. The boundary condition far upstream (at $z \rightarrow \infty$ for $u_+ > 0$) is enforced by restricting the expansion to $i < 0$; that far downstream is imposed by requiring the projection onto downstream eigenfunctions with $i > 0$ to vanish, thus preventing divergence of the distribution as $z \rightarrow -\infty$.

In the case of parallel, relativistic shocks, the expansion (13) was found to converge rapidly, and an accurate result was obtained by retaining only a single eigenfunction (Kirk et al. 2000). The current problem is more complicated, since the eigenfunctions are functions of gyro-phase ϕ as well as pitch angle θ , and the eigenvalue problem changes from a single-parameter (u_s) problem into a two-parameter (u_s, η) problem. This makes an expansion to high order cumbersome. Also, the differential operator in (14) is not self-adjoint, so that the adjoint operator (obtained by changing the sign of the $\partial/\partial\phi$ term) must be used to find the function needed for projection onto the “forbidden” downstream eigenfunction. Nevertheless, the analogy is close, so that one can again hope to find a reasonable approximation by using only a single eigenfunction. Adopting this approach, the power-law index s for a shock moving at speed u_+ into the upstream fluid and at speed u_- in the downstream fluid is given implicitly by the equation

$$S \equiv \iint d\mu_- d\phi_- \bar{Q}_-(\mu_-, \phi_-) (v_{z-} - u_-) \times (p_+/p_-)^{-s} Q_+(\mu_+, \phi_+) = 0 \quad (15)$$

where the label $i = -1$ of the retained, leading eigenfunction has been omitted, and the notation \bar{Q} is used to denote the corresponding eigenfunction of the adjoint equation. The notation (μ_{\pm}, ϕ_{\pm}) is used to indicate angles in the up and downstream fluid frames. For particles that move rapidly with respect to the shock, (15) can be expanded to first order in u/v , leading to a linear equation for s , with solution:

$$s \approx \frac{1}{(u_+ - u_-)} \times \frac{\iint d\mu_- d\phi_- \bar{Q}_-(\mu_-, \phi_-) (v_{z-} - u_-) Q_+(\mu_+, \phi_+)}{\iint d\mu_- d\phi_- \bar{Q}_-(\mu_-, \phi_-) v_{z-}^2 Q_+(\mu_+, \phi_+)} \quad (16)$$

where, for simplicity, the relative speed of the downstream fluid with respect to the upstream fluid is assumed to be $u_+ - u_-$, implying that they both flow along the shock normal, which is the case for a shock of high Alfvénic mach number (see, for example, Kirk & Heavens 1989).

The retained eigenfunction with $i = -1$ is special in

two respects. Firstly, since it falls off more slowly with distance from the shock than do the other eigenfunctions, it is the dominant contribution to the distribution function far upstream, and so can have no zeroes in the range $0 < \phi < 2\pi$, $-1 < \mu < 1$. Secondly, in the limit $u \rightarrow 0$, it merges with the eigenfunction $i = 0$, which is a well-known feature characteristic of the diffusion approximation (Fisch & Kruskal 1980). Taking this limit, it is straightforward to show that both Λ_{-1} and the anisotropic part of Q_{-1} are of first order in u . The transformation of the arguments of the eigenfunction Q_+ in equation (16) from μ_+, ϕ_+ to μ_-, ϕ_- acts on the anisotropic part of this function only. In the case of highly relativistic particles, to which we restrict ourselves in the following, it produces a modification of this term that is of first-order in $(u_+ - u_-)$. It follows that

$$Q_+(\mu_+, \phi_+) = Q_+(\mu_-, \phi_-) + O(u_+^2) \quad (17)$$

and, using the orthogonality relations

$$\iint d\mu_+ d\phi_+ (v_{z+} - u_+) \bar{Q}_- = 0 \quad (18)$$

$$\iint d\mu_- d\phi_- (v_{z-} - u_-) Q_+ = 0 \quad (19)$$

in equation (16), leads immediately to the standard DSA result (3).

However, this analysis is based on the assumption that u is the only small parameter in the problem, which breaks down when scattering is sufficiently weak. Assuming the ordering $u \sim 1/\eta \sim \epsilon \ll 1$, standard perturbation techniques (for details see appendix A) lead to an expression for Q that is anisotropic at zeroth order:

$$Q = a(\mu) e^{\Lambda v \sqrt{1-\mu^2} \cos \phi} + O(\epsilon) \quad (20)$$

where

$$a(\mu) = \text{Ps}_0^0(\mu, -\Lambda^2/2) \quad (21)$$

with Ps_0^0 the angular, oblate, spheroidal wave function with $m = n = 0$ (in the notation of Thompson 2011, chapter 30). The eigenvalue Λ is related to the spheroidal eigenvalue λ_0^0 by

$$\lambda_0^0(-\Lambda^2/2) = \Lambda(\Lambda + 2\eta u) \quad (22)$$

and is of zeroth order in ϵ .

Evaluation of the ϕ integrals in (16) is straightforward. The integrals over μ do not appear to be possible analytically, but are simple numerical quadratures. An expansion in powers of ηu yields

$$s = \frac{3r}{r-1} + \frac{9(r+1)}{20r(r-1)} \eta^2 u_+^2 + O(\eta^4 u_+^4) \quad (23)$$

indicating a significant softening of the spectrum for finite ηu_+ , as compared to the standard DSA result. In section 5 we compare this result and the angular dependence of the eigenfunction defined by equations (20) and (21) with the results of the Monte-Carlo simulations described below.

4. MONTE-CARLO SIMULATIONS

To solve the fully relativistic kinetic equation (1), we use two conceptually different, but closely related Monte-Carlo methods, similar to those described by

Achterberg et al. (2001) and by Ellison & Double (2004) and Summerlin & Baring (2012).

In the first, we rewrite (1) in the form of a Fokker-Planck equation, and use a theorem due to Itoh (1944) to write down a stochastic differential equation governing a family of effective trajectories, whose statistical properties are those of the required solution f (see Gardiner 1994, chapter 4). An explicit first-order discretization scheme is then used to construct a large number of these trajectories. In the second, we start from the Boltzmann equation describing a distribution of particles that move in the unperturbed, uniform magnetic field, but are subject to random collisions, each of which causes a small but finite angular deflection. In the limit of small and frequent deflections this equation can be reduced to (1), as we demonstrate in Appendix C. but we solve it for small finite deflections, advancing the trajectory in between the scatterings by numerical integration. Details are provided in Appendices B and C. We have verified that the results presented in Section 5 do not depend on which algorithm is employed.

In each case, trajectories are initiated at the shock front. They then perform an excursion that either returns it to the shock, or terminates the trajectory when it crosses a boundary placed at a large, fixed (in units of the gyro-radius r_g) distance from the shock front in the downstream region. An excursion that returns to the shock front initiates a subsequent excursion in the other half-space, starting at the same space-time point with the same space-time coordinates and momentum four vector.

The anisotropy of the particle distribution at the shock front is the characteristic feature of this problem. In addition, we are interested in two properties of the solutions: the time-asymptotic power-law index at momenta well above injection, and the mean time taken for acceleration to a given momentum. These quantities can be used to determine whether or not a SNR lives long enough to enable acceleration at quasi-perpendicular shocks to play an important role. Each of them can be extracted from a simulation of a large number of trajectories, all injected at momentum p_0 (assumed $\gg mc$) at time $t = 0$, by recording the sets of values t_i and p_i at each crossing of the shock front. These values, collectively called *events*, are labeled by the integer i .

The distribution at the shock front as a function of the angles θ and ϕ , and the momentum p (in each case integrated over the other two variables) is obtained by setting up logarithmically spaced bins, and adding to these a weighting factor equal to the reciprocal of the relative velocity of the particle with respect to the shock surface. Particles are initiated at the shock with an angular distribution that is arbitrarily chosen to be isotropic in the hemisphere entering the upstream plasma. However, after a few shock crossings, the bias thereby introduced is lost, and the distribution settles down to one that is independent of the number of crossings, and can be compared to the analytical form found for the scale-free, power-law distribution. Provided the average number of crossings per trajectory is large (in the example presented below it is roughly 100) the effect of the bias is not noticeable. After a few crossings, particles display a power spectrum which extends from slightly above p_0 up to a momentum determined by the position of the downstream boundary, or the time limit placed on the trajectory. Within this

range, the time-asymptotic power-law index s is found from a least-squares fit in log-log space. To find the average acceleration time, the events are again binned in p , and, at the same time, a running average of t_i is accumulated. In the results presented below, s and t_i were determined using the range $0.1 < \log_{10}(p/p_0) < 1$.

5. RESULTS

We present the results of fully relativistic simulations of perpendicular shocks for an upstream speed u_s ($\equiv u_+$) ranging from 0.01 to 0.2 (in units of c), and a turbulence parameter η between 1 and 100, and compare them to analytic approximations. A total of 50,000 trajectories were simulated for each set of parameters. For convenience, the plasma is assumed to flow along the shock normal both upstream and downstream, and the compression ratio $r = u_+/u_-$ is chosen to equal 4, which corresponds approximately to the value derived from the Rankine-Hugoniot conditions for an ideal gas of specific heat ratio 5/3, (although it is not relativistically exact for any physically motivated equation of state). The magnetic field strengths B_+ and B_- , measured in the up and downstream rest frames, respectively, are related by $B_+/B_- = r\Gamma_s\sqrt{1 - (u_s/r)^2}$ (see Kirk & Heavens 1989, eq (4)). Itoh's method was used in the simulations presented here.

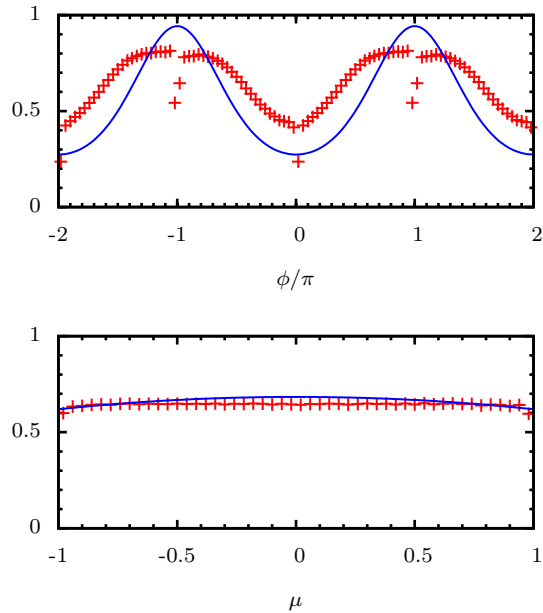


Figure 1. The angular dependence of the distribution function f at the shock (arbitrary normalization) for $u_s = 0.012$ and $\eta = 22$. Monte-Carlo simulations (red points) are compared to zeroth-order analytic approximations. The top panel shows the phase dependence, (f integrated over pitch angle), the bottom panel the pitch angle dependence, (f integrated over phase). The blue lines are found by integrating the expression given in equation (20) numerically.

Figure 1 shows the angular distribution at the shock front found from Monte-Carlo simulation as a function of gyro-phase ϕ (top panel) and cosine μ of the pitch angle (bottom panel), for upstream speed $u_s = 0.012$ and turbulence level $\eta = 22$ ($\eta u_s = 0.26$). Particles are registered by the simulation as they cross the shock front,

so that very few events accumulate in bins where the velocity vector lies close to the plane of the shock, i.e., at $\sqrt{1 - \mu^2} \sin \phi \approx u_s$. This accounts for the relatively large fluctuations close to $\phi = 0, \pm\pi$, which corresponds to grazing incidence for most values of μ . The maximum of the distribution function lies close to $\phi = \pm\pi$, which corresponds to particles moving along the shock front in the direction of the shock- or “grad-B”- drift. The zeroth-order analytic approximation reproduces the main features of the simulated distributions, although it is more strongly peaked both in ϕ . This may be either because the eigenfunction expansion requires several terms in order to converge to an accurate solution, and/or because the analytic approximation is, strictly speaking, valid only in the limit of nonrelativistic shocks and low scattering rates ($u_s \sim 1/\eta \rightarrow 0$). In any case, it is clearly important to employ a scattering algorithm in the simulations that resolves angular structure on the small scale indicated by the eigenfunction.

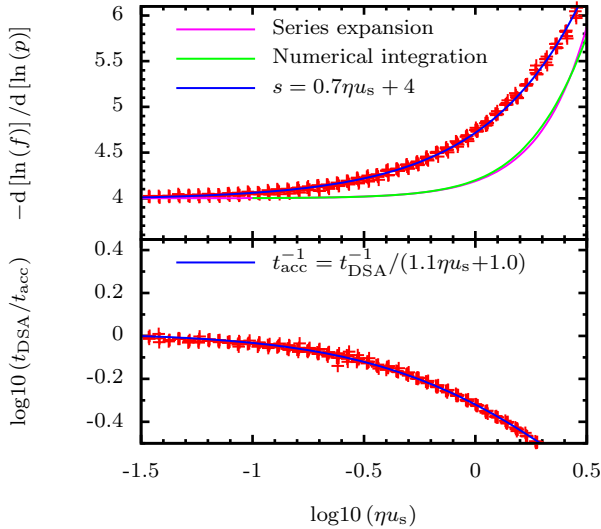


Figure 2. The energy spectral index s (top panel) and the acceleration rate divided by the DSA prediction (bottom panel), as a functions of ηu_s . Red crosses show the results that fall in the plotted range of Monte-Carlo simulations with 10 values of η , between 1 and 100, and 30 values of u_s between 0.01 and 0.2, in each case equally spaced in logarithms. Cyan and green curves in the top panel show analytic approximations using the series expansion given in equation (23), and numerical integration respectively. Blue curves show fits to the simulation results.

Figure 2 shows the time-asymptotic power-law index s (top panel) and the average acceleration rate (bottom panel) at a perpendicular shock front, as functions of the product ηu_s , for various values of the parameters u_s and η . In each case, the results fall close to a single curve with very small dispersion about it. This suggests that the most important parameter in this range is the combination ηu_s , which is also the only parameter of the approximate solutions found in section 3. Physically, ηu_s is the collision time divided by the time taken for the upstream flow to travel across one particle gyro-radius, i.e., roughly the inverse of the number of collisions expected

as an undisturbed particle orbit advects across the shock. Provided the fluid speed is nonrelativistic, this is the only physically significant dimensionless quantity in the problem as we formulate it.

For $\eta u_s \ll 1$, the Monte-Carlo simulations show a spectral index s that lies close to the DSA prediction $s = 4$, in agreement with the analytic approximations. The acceleration rate in this regime is also close to the DSA prediction, which is a factor $2.5\eta(1 + 1/\eta^2)$ faster than the Bohm rate, as defined in equation (10). Inspection of the angular distributions shows, as expected, that they are almost isotropic in this region.

However, as ηu_s increases, simulations show that the index s increases (i.e., softens). This is also seen in the analytic approximations, although the softening here sets in at somewhat higher ηu_s , and proceeds more rapidly. According to the simulation results, a softening of unity, i.e., $s = 5$ is reached at $\eta u_s \approx 1$, whereas the zeroth-order analytic approximation predicts this index at $\eta u_s \approx 2$. The softening of the spectrum is accompanied by a reduction in the acceleration rate, expressed in units of the DSA-predicted rate. At $\eta u_s = 1$, the reduction is roughly a factor 2, implying that acceleration still proceeds at a rate that is about a factor of η faster than the Bohm rate.

6. DISCUSSION

The results presented above demonstrate that perpendicular shocks impose a strong anisotropy on particles that are scattered in the upstream and downstream plasma, when the ratio $1/\eta$ of the scattering rate to the gyro frequency is less than or of the order of the ratio of the shock speed to the particle speed. Instead of diffusing in space around the shock front, as predicted by DSA, the accelerated particles are then concentrated into a fan-beam structure within a relatively small interval $\Delta\phi$ of gyro-phase directed in the plane of the shock. This can be seen from the phase-dependence of the eigenfunction given in equation (20): $Q \propto \exp[\Lambda v \sqrt{1 - \mu^2} \cos \phi]$. The direction of the beam corresponds to the drift imposed on an unscattered trajectory by the presence of the shock front. For $\eta u_s > 1$, the opening angle of the fan beam can be estimated from the asymptotic expression for the eigenvalue, $\Lambda \sim -3\eta u_s$ (see Appendix A), to be $\Delta\phi \sim (\eta u_s)^{-1/2}$. This roughly corresponds to the diffusive spread in phase produced by the scattering operator in equation (1), when acting on a perfectly collimated beam over the time ($\approx 1/(\omega_g u_s)$) taken for an unperturbed trajectory to cross the shock.

In this regime, a particle that is moving close to the shock front on its downstream side which finds itself inside the fan beam has a relatively high probability of recrossing the shock front many times. On the other hand, a particle in the same position but with a momentum directed out of the beam is likely to be swept away downstream after only a few crossings. For this reason, the intuitive picture of DSA, which is based on assigning all accelerated particles in the downstream plasma an escape probability that is independent of their position and direction of motion, is inadequate. The more formal derivation of DSA based on the diffusion-advection equation also breaks down, because spatial diffusion describes the transport process only when the distribution

is approximately isotropic.

We find that the gradual breakdown of DSA at a non-relativistic, perpendicular shock as the collision rate decreases depends on the single parameter ηu_s and has two important effects on the accelerated particles. Firstly, it softens the spectrum. For a compression ratio of 4, the phase-space density, $f \propto p^{-s}$, has $s \approx 0.7\eta u_s + 4$, compared to the DSA prediction of $s = 4$. Secondly, it causes a reduction in the acceleration rate by a factor of approximately $1.1\eta u_s + 1$ compared to the DSA prediction, which rises linearly with η . Thus, optimal conditions for acceleration, in the sense that it proceeds rapidly and produces a reasonably hard particle spectrum, are found when the anisotropies induced by the shock speed and the magnetic compression are comparable, i.e., when $\eta u_s \approx 1$.

The validity of DSA at perpendicular shocks has been a controversial issue for many years. Jokipii (1987) suggested that breakdown would happen when the collision time becomes longer than the time during which a gyrating particle interacts with the shock, leading to the approximate condition $\eta < 1/u_s$ and an upper limit on the acceleration rate that is first order in ϵ :

$$\begin{aligned} t_{\text{acc}}^{-1} &< 1/(u_s t_B) \\ &= u_s \frac{r-1}{r} \omega_g \\ &\sim \mathcal{O}(\epsilon) \omega_g. \end{aligned} \quad (24)$$

This estimate is in rough agreement with our findings. Achterberg & Ball (1994), on the other hand, proposed that the collision frequency must be large enough to allow particles to diffuse along the magnetic field whilst upstream of the shock. This leads to the restriction $\eta < 1/\sqrt{u_s}$ and

$$\begin{aligned} t_{\text{acc}}^{-1} &< u_s^{-1/2} t_B^{-1} \\ &= u_s^{3/2} \frac{r-1}{r} \omega_g \\ &\sim \mathcal{O}(\epsilon^{3/2}) \omega_g. \end{aligned} \quad (25)$$

Our result that the acceleration time and spectral index are functions of the product ηu_s does not support this conjecture. However, the situation may be different at oblique shocks, where particles have more opportunity to diffuse along the upstream magnetic field lines.

The importance of these effects for the acceleration of high energy cosmic rays has been emphasized in particular by Jokipii (1987) and by Biermann (1993). Nevertheless, cosmic-ray acceleration at quasi-perpendicular shocks has received relatively little attention for several reasons. Firstly, observations of the polarization of radio emission in SNR 1006 show that accelerated electrons are found predominantly in regions where the magnetic field is disordered, and where the normal to the shock front lies roughly in the direction of the external field, rather than perpendicular to it (Reynoso et al. 2013). This general trend is also consistent with the predominantly radial orientation of the interior magnetic field in young supernova remnants (Reynolds & Gilmore 1993; Parizot et al. 2006; Reynolds et al. 2012), and fits in with the idea that magnetic field generation acts at quasi-parallel shocks. Secondly, numerical simulations

of acceleration using Monte-Carlo codes (Ellison et al. 1995; Ellison & Double 2004; Summerlin & Baring 2012), hybrid codes (Caprioli & Spitkovsky 2014), and PIC codes (Stockem et al. 2012; Sironi et al. 2013; Matsumoto et al. 2013) also disfavor the quasi-perpendicular orientation, which, according to these results, is less efficient at injecting particles into the acceleration process, provided the initial level of turbulence is very low.

However, these reasons do not directly apply to the problem of the acceleration of very high energy ions, on which we focus our attention in this paper. On the one hand, observations of synchrotron radiation relate exclusively to the electron distribution, which is likely to be much more tightly confined to the shock front than are high-energy ions. On the other, numerical simulations consider an initially uniform upstream magnetic field. This may indeed inhibit injection, but, in a more realistic situation, some level of turbulence must be present initially. Our results indicate that efficient acceleration can be expected for an effective collision frequency $\nu_{\text{coll}} \sim u_s \omega_g$, which implies a very low level of turbulence under SNR conditions. However, if the collision frequency is even lower, we find that perpendicular shocks should produce only very steep spectra, in agreement with the apparent failure of these shocks to trigger acceleration in numerical simulations. Furthermore, in a realistic situation, low energy particles may see localized regions of quasi-parallel geometry due to small length-scale fluctuations in the upstream medium and/or the shock speed. These regions may be very effective accelerators, possibly giving rise to substantial field amplification. But, as described by Bell (2014) the affected acceleration region remains limited in spatial extent, and automatically provides an escaping flux of particles at the highest energy to which it operates. In the context of the problem we consider here, these can be regarded as being injected into an acceleration process operating on larger spatial scales, on which the shock is perpendicular.

Another well-known argument against acceleration to energies above the knee at perpendicular shocks is that particles drift across the shock surface whilst undergoing acceleration, covering a distance proportional to their energy. Depending on the geometry of the field, this might move them out of the region where the shock is perpendicular. If one sets an upper limit to this distance equal to the radius of the SNR, the corresponding upper limit on the energy turns out to be comparable to that found for quasi-parallel shocks (e.g., Bell 2014), and is roughly equal to the energy a particle could gain by drifting from the pole to the equator (or vice versa) in a flow moving at the shock speed through a steady, magnetized, axisymmetric stellar wind.

However, whether or not particle drift really limits the maximum energy depends on the specific configuration of the magnetic field. For example, in a uniform external field the drift motion induced by a spherical shock front is directed along lines of constant latitude (measured on the shock surface with the polar axis along the direction of the external magnetic field), along which the shock does not change its obliquity. Diffusion along the magnetic field lines in this configuration might allow particles to escape to regions where the shock is parallel, but this effect depends on the transport properties in the up-

stream and downstream plasmas, rather than on the drift motion.

The situation is different for a spherical shock front expanding into a magnetic field that is anchored in the wind of a rotating progenitor star. In the ideal case of a magnetic dipole aligned with the rotation axis, a small region with quasi-parallel configuration may exist close to the axis. However, if the progenitor is a miss-aligned rotator, and/or one that undergoes repeated field reversals, the undisturbed field is perpendicular to the shock normal essentially everywhere, once this has expanded to well beyond the Alfvén radius. In this case, the direction in which a particle drifts as the shock moves over a magnetic field that is frozen into the progenitor’s wind, can be a rapidly changing function of the shock radius.

The majority of supernovae are thought to result from the explosion of massive stars that can be assumed to have had a strong wind, and may have been both magnetized and rapidly rotating. Assuming a wind speed of v_w , and an Alfvén surface not too far from the star, the toroidal magnetic field at large radius R can be estimated as $B(R) = B_* (\Omega R_*/v_w) (R_*/R)$, where R_* is the stellar radius, B_* the surface magnetic field and Ω the angular velocity of the star (Parker 1958). Then, defining the maximum energy E_{\max} to which a proton can be accelerated by identifying the acceleration rate given in equation (11) with $u_s c/R$, setting $r = 4$, and inserting values thought typical of Wolf-Rayet stars (Berezhko & Völk

2000), leads to

$$\begin{aligned} E_{\max} &= \frac{3}{8} \eta u_s \left(\frac{R_* \Omega}{v_w} \right) e B_* R_* \\ &= 1.7 \cdot 10^{16} \eta u_s \left(\frac{R_* \Omega}{v_w} \right) \left(\frac{B_*}{50 \text{ G}} \right) \left(\frac{R_*}{3 \cdot 10^{12} \text{ cm}} \right) \text{ eV}, \end{aligned} \quad (26)$$

We find that equation (11) over-estimates the acceleration rate by a factor of 2 when $\eta u_s \approx 1$, which is unimportant in view of the uncertain values of Ω and B_* . Therefore, we conclude that, under optimal conditions, i.e., when $\eta u_s \approx 1$, such objects may be capable of accelerating protons into a power-law spectrum somewhat softer than that predicted by DSA up to energies well in excess of 1 PeV.

7. CONCLUSIONS

We have studied the distribution function of particles accelerated at perpendicular shocks as their scattering rate decreases, finding that a strong anisotropy develops, which causes the theory of diffusive shock acceleration to fail. When the scattering time is comparable to the time taken for a particle orbit to traverse the shock front, the power-law index of the particle distribution is found to soften by roughly unity, compared to the DSA prediction and the acceleration rate is roughly halved. These results provide a firm basis in kinetic theory for the long-standing conjecture that protons can be accelerated to energies well above 1 PeV at the perpendicular shocks that are expected to form when a supernova explodes into the wind of a massive progenitor.

We thank the anonymous referee for a very helpful report. This work is supported in part by the Postdoctoral Fellowships for Research Abroad program by the Japan Society for the Promotion of Science No. 20130253 and by the Research Fellowship for Young Scientists (PD) by the Japan Society for the Promotion of Science No. 20156571 (M.T.). M.T. also thanks the Theoretical Astrophysics group at the Max-Planck-Institut fuer Kernphysik for their hospitality.

APPENDIX

APPROXIMATE ANALYTIC SOLUTION

In equation (14) we assume $u \sim 1/\eta \sim \epsilon \ll 1$, reintroduce the label i , and pose an expansion:

$$Q_i \rightarrow Q_i^{(0)} + \epsilon Q_i^{(1)} + O(\epsilon^2) \quad (A1)$$

$$\Lambda_i \rightarrow \Lambda_i^{(0)} + \epsilon \Lambda_i^{(1)} + O(\epsilon^2). \quad (A2)$$

Since $v_z = v \sqrt{1 - \mu^2} \sin \phi$, the zeroth order terms

$$\frac{\partial Q_i^{(0)}}{\partial \phi} + \Lambda_i^{(0)} v_z Q_i^{(0)} = 0 \quad (A3)$$

can be integrated to give (writing $\mu = \cos \theta$ where it makes the notation more compact):

$$Q_i^{(0)} = a_i(\mu) e^{\Lambda_i^{(0)} \sin \theta \cos \phi} \quad (A4)$$

and, for the adjoint function

$$\bar{Q}_i^{(0)} = \bar{a}_i(\mu) e^{-\Lambda_i^{(0)} \sin \theta \cos \phi}. \quad (A5)$$

The first order terms are:

$$\left[\frac{\partial}{\partial \phi} + \Lambda_i^{(0)} \sin \theta \sin \phi \right] Q_i^{(1)} = \left(\Lambda_i^{(0)} u - \Lambda_i^{(1)} \sin \theta \sin \phi \right) Q_i^{(0)} + \frac{1}{2\eta} \left[\frac{\partial}{\partial \mu} (1 - \mu^2) \frac{\partial}{\partial \mu} + \frac{1}{1 - \mu^2} \frac{\partial^2}{\partial \phi^2} \right] Q_i^{(0)}. \quad (\text{A6})$$

Integrating, using the integrating factor $e^{-\Lambda_i^{(0)} \sin \theta \cos \phi}$ gives

$$Q_i^{(1)} = e^{\Lambda_i^{(0)} \sin \theta \cos \phi} \left[\int_0^\phi d\phi' F(\phi') + \frac{1}{4\eta} b(\mu) \right] \quad (\text{A7})$$

$$F(\phi) = e^{-\Lambda_i \sin \theta \cos \phi} \left[\left(\Lambda_i^{(0)} u - \Lambda_i^{(1)} \sin \theta \sin \phi \right) Q_i^{(0)} + \frac{1}{2\eta} \left(\frac{\partial}{\partial \mu} (1 - \mu^2) \frac{\partial}{\partial \mu} + \frac{1}{1 - \mu^2} \frac{\partial^2}{\partial \phi^2} \right) Q_i^{(0)} \right]. \quad (\text{A8})$$

Imposing periodic boundary conditions in ϕ , on $Q^{(1)}$ leads to

$$\frac{\partial}{\partial \mu} (1 - \mu^2) \frac{\partial a_i}{\partial \mu} + \frac{\Lambda_i^{(0)}}{2} \left(\Lambda_i^{(0)} (1 + \mu^2) + 4\eta u \right) a_i = 0, \quad (\text{A9})$$

which is to be solved with boundary conditions

$$\frac{da_i}{d\mu} = \mp \frac{\Lambda_i^{(0)}}{2} \left(\Lambda_i^{(0)} + 2\eta u \right) a_i \quad \text{at } \mu = \pm 1. \quad (\text{A10})$$

The first-order terms are then:

$$Q_i^{(1)} = \frac{e^{\Lambda_i^{(0)} \sin \theta \cos \phi}}{4\eta} \left\{ b + 4\eta \Lambda_i^{(1)} \sin \theta (\cos \phi - 1) a_i - \Lambda_i^{(0)} \sin \theta \sin \phi \left[\left(4 + \Lambda_i^{(0)} \sin \theta \cos \phi \right) a_i + 4 \cos \theta \frac{da_i}{d\mu} \right] \right\} \quad (\text{A11})$$

$$\bar{Q}_i^{(1)} = \frac{e^{-\Lambda_i^{(0)} \sin \theta \cos \phi}}{4\eta} \left\{ b - 4\eta \Lambda_i^{(1)} \sin \theta (\cos \phi - 1) a_i - \Lambda_i^{(0)} \sin \theta \sin \phi \left[\left(4 - \Lambda_i^{(0)} \sin \theta \cos \phi \right) a_i + 4 \cos \theta \frac{da_i}{d\mu} \right] \right\} \quad (\text{A12})$$

where $b \sim 1$ and $\bar{b} \sim 1$ are functions of μ which, together with $\Lambda_i^{(1)}$, can be constrained by examining the second order equations. However, because these terms are even in ϕ , they do not enter into the computation of the index s .

Equation (A9) is a special case of the spheroidal differential equation (Thompson 2011, chapter 30), whose solutions, for real Λ_i , are the oblate, angular, spheroidal wave functions $\text{Ps}_n^m(\mu, -\Lambda_i^2/2)$. In general, solutions exist for both positive and negative Λ_i , together with the special isotropic solution $\Lambda_0 = 0$, $a_0 = \text{constant}$. However, to represent the upstream distribution we require an eigenfunction which has no roots for $-1 < \mu < 1$. This is the function $\text{Ps}_0^0(\mu, -\Lambda_{-1}^2/2)$. The eigenvalues of the spheroidal wave equation $\lambda_n^m(\gamma^2)$ (in the notation of Thompson (2011)) are defined for $n \geq m$ and ordered such that $\lambda_n^m < \lambda_{m+1}^m < \dots$. They are related to Λ_i by

$$\lambda_{-i-1}^0(-\Lambda_i^2/2) = \Lambda_i (\Lambda_i + 2\eta u) \quad . \quad (\text{A13})$$

Thus, as expected, the largest negative eigenvalue Λ_{-1} corresponds to λ_0^0 and, therefore, to the eigenfunction that has no roots in the range $-1 < \mu < 1$. For large $\eta\mu$, $\Lambda_{-1} \rightarrow -2\eta u$. A power series in ηu , can be found directly from (A9) (see also Meixner & Schäfke 1954, p 240):

$$\Lambda = -3\eta u + \frac{3}{20} (\eta u)^3 + \text{O}(\eta^5 u^5) \quad (\text{A14})$$

$$a = 1 + \frac{3}{4} \mu^2 (\eta u)^2 + \frac{3}{160} \mu^2 (4 + 9\mu^2) (\eta u)^4 + \text{O}(\eta^6 u^6) \quad (\text{A15})$$

Using these series to evaluate the integrals in equation (16) leads to equation (23).

MONTE-CARLO METHOD BASED ON STOCHASTIC DIFFERENTIAL EQUATIONS

Equation (1), when rewritten in Fokker-Planck form, becomes:

$$\frac{\partial f}{\partial t} = -\frac{\partial}{\partial \vec{x}}(\vec{v}f) + \frac{\partial}{\partial \mu}\left(\frac{\mu f}{\eta}\right) - \frac{\partial}{\partial \phi}f + \frac{\partial^2}{\partial \mu^2}\left(\frac{(1-\mu^2)f}{2\eta}\right) + \frac{\partial^2}{\partial \phi^2}\left(\frac{f}{2\eta(1-\mu^2)}\right) \quad (\text{B1})$$

where $\mu = \cos\theta$, time and space are measured in units of ω_g^{-1} and c/ω_g , and \vec{v} is in units of c . Solutions to this equation can be found by constructing sample trajectories that satisfy the set of stochastic differential equations (see Gardiner 1994)

$$\begin{aligned} d\vec{x} &= \vec{v}dt \\ d\mu &= -(\mu/\eta)dt + [(1-\mu^2)/\eta]^{1/2}dW_t \\ d\phi &= dt + [(1-\mu^2)\eta]^{-1/2}dW_t \end{aligned} \quad (\text{B2})$$

where dW_t is an infinitesimal Wiener process. We use an explicit first-order discretization to find a numerical solution to this set, consisting, for each sample trajectory, of a sequence of points in phase space labeled by i :

$$\begin{aligned} \vec{x}_{i+1} &= \vec{x}_i + \vec{v}_i\Delta t \\ \mu_{i+1} &= \mu_i - (\mu_i/\eta)\Delta t + \xi_i\sqrt{\frac{\Delta t(1-\mu_i^2)}{\eta}} \\ \phi_{i+1} &= \phi_i + \Delta t + \zeta_i\sqrt{\frac{\Delta t}{(1-\mu_i^2)\eta}} \end{aligned} \quad (\text{B3})$$

where ξ_i and ζ_i are random numbers uniformly distributed on the interval $(-\sqrt{3}, \sqrt{3})$, which, therefore, have zero mean and unit variance. This scheme is rapid, but has the disadvantage that trajectories that pass very close to the points $\mu = \pm 1$ are subject to errors. The affected range depends on the time-step, and is given approximately by $|\mu| > 1 - \Delta t/\eta$. Typically, we choose $\Delta t = 10^{-2}$ and $1 < \eta < 20$, so that $\lesssim 1\%$ of particles in an isotropic distribution are affected. This is unimportant in the simulations presented above, where no fine-scale structure in μ is expected. However, it could become a concern for parallel, relativistic shocks with $\Gamma \gtrsim 100$.

Each sample trajectory starts on the shock front and consists of a series of excursions into the up and downstream plasmas, ending when it crosses a boundary placed a fixed distance d downstream of the shock. We performed simulations for several different values of d . For oblique shocks, $d \sim 200$ is sufficient, in the sense that a power-law distribution in p is reproduced over several decades. However, parallel shocks require $d \sim 1000$, reflecting the fact that the diffusion length along the magnetic field is greater than that across it, if $\eta > 1$. When a timestep causes a trajectory to cross the shock front, the step is repeated with smaller Δt chosen to place the particle precisely on the shock front. The total number of timesteps in the excursion is then checked, and the excursion repeated if this number is too small — typically less than 3. This procedure eliminates trajectories that depend strongly on the finite size of the timestep, at the expense of distorting the angular distribution of particles at the shock front that move almost tangential to it, thereby limiting the ability of the simulation to resolve fine-structure in gyro-phase ϕ in directions close to the plane of the shock. From the analytic approximation, such structure should be present on the scale $\Delta\phi \sim 1/\Lambda \sim (\eta u_s)^{-1}$, so that the choice $\Delta t = 1/100$ limits the accessible parameter range to $\eta u_s < 100$.

MONTE-CARLO METHOD BASED ON THE BOLTZMANN EQUATION

In this method we solve the equation that results when the right-hand side of equation (1) is replaced by the Boltzmann collision operator corresponding to elastic pitch-angle scattering in the test particle approximation, given by

$$\left(\frac{\partial f}{\partial t}\right)_{\text{coll}} = \frac{1}{t_{\text{scatt}}} \left[\frac{1}{2\pi} \int_{-1}^1 \int_0^{2\pi} d\mu' d\phi' f(\mu', \phi') p(\mu, \phi; \mu', \phi') - f(\mu, \phi) \right], \quad (\text{C1})$$

where t_{scatt} is the mean time between scatterings and $p(\mu, \phi; \mu', \phi')$ is the probability that a particle with (μ', ϕ') is scattered into (μ, ϕ) in a single scattering. This equation is solved using the method developed by Ellison & Eichler (1984); Jones & Ellison (1991); Ellison & Double (2004). Trajectories whose statistical properties are given by f are found by numerically integrating the standard relativistic equations of motion in a steady background electromagnetic field — corresponding to the left-hand side of equation (1) — using the exact solution or the Bulirsh-Stoer method over a fixed time interval chosen to equal the average time between scatterings: $t_{\text{scatt}} = 2\pi/\omega_g N$, where $N (\gg 1)$ is a parameter of the scattering model. (Formally, a random, exponentially distributed time interval with mean value t_{scatt} should be employed, but this is not necessary in the present problem, where the number of scatterings between each encounter with the shock is required to be large). On scattering, trajectories are subject to a random deflection through a small angle that is uniformly distributed between zero and Θ_{max} (for details see Summerlin & Baring (2012)). This

enables one to identify a timescale t_{iso} on which the particle distribution would, in the absence of a driving mechanism, relax to isotropy:

$$t_{\text{iso}} = 6t_{\text{scatt}}/\Theta_{\text{max}}^2 \quad (\text{C2})$$

The equation of motion is solved in the upstream and downstream half-spaces in the respective comoving frame, allowing the sample trajectories to cross the shock front without deflection or energy change. The escape boundary is located in the downstream region where the probability of particles returning to the shock front is sufficiently small, as described in Appendix B.

In order to demonstrate the link between this method and the stochastic differential equation approach described in appendix B, we note that when the limit $N \rightarrow \infty$ is taken with t_{iso} fixed, the scattering model corresponds to a phase function

$$\begin{aligned} p(\mu, \phi; \mu', \phi') &= p(\cos \Theta) \\ &= H(\cos \Theta_{\text{max}} - \cos \Theta) / (2\pi \Theta_{\text{max}} \Theta), \end{aligned} \quad (\text{C3})$$

where we assume $\Theta \ll 1$ and use the normalization $\iint d\phi d\Theta \sin \Theta p(\cos \Theta) = 1$. Expanding this phase function by writing

$$p(\cos \Theta) = 4\pi \sum_{n=0}^{\infty} \sum_{m=-n}^n \sigma_n Y_n^m(\theta, \phi) Y_n^{m*}(\theta', \phi'), \quad (\text{C4})$$

where Y_n^m is a spherical harmonic, and the asterisk means the complex conjugation, one finds

$$\sigma_n = \frac{1}{2} \left[1 - \frac{\Theta_{\text{max}}^2}{12} n(n+1) \right]. \quad (\text{C5})$$

Using equations (C4) and (C5), the collision operator, equation (C1), can be rewritten as follows:

$$\left(\frac{\partial f}{\partial t} \right)_{\text{coll}} = -\frac{\Theta_{\text{max}}^2}{12t_{\text{scatt}}} \int_{-1}^1 \int_0^{2\pi} d\mu' d\phi' \left[\sum_{n=0}^{\infty} \sum_{m=-n}^n n(n+1) Y_n^m(\theta, \phi) Y_n^{-m}(\theta', \phi') \right] f(\mu, \phi) \quad (\text{C6})$$

where we used the completeness relation:

$$\sum_{n=0}^{\infty} \sum_{m=-n}^n Y_n^m(\theta, \phi) Y_n^{-m}(\theta', \phi') = \delta(\mu - \mu') \delta(\phi - \phi'). \quad (\text{C7})$$

Furthermore, using the following two relations:

$$-n(n+1)Y_n^m = \left[\frac{\partial}{\partial \mu}(1-\mu^2) \frac{\partial}{\partial \mu} + \frac{1}{1-\mu^2} \frac{\partial^2}{\partial \phi^2} \right] Y_n^m, \quad (\text{C8})$$

$$\begin{aligned} \int_{-1}^1 \int_0^{2\pi} d\mu d\phi f(\mu) Y_n^m &= -\frac{1}{n(n+1)} \int_{-1}^1 \int_0^{2\pi} d\mu d\phi Y_n^m \\ &\times \left[\frac{\partial}{\partial \mu}(1-\mu^2) \frac{\partial}{\partial \mu} + \frac{1}{1-\mu^2} \frac{\partial^2}{\partial \phi^2} \right] f, \end{aligned} \quad (\text{C9})$$

the collision operator finally becomes:

$$\left(\frac{\partial f}{\partial t} \right)_{\text{coll}} = \frac{1}{2t_{\text{iso}}} \left[\frac{\partial}{\partial \mu}(1-\mu^2) \frac{\partial}{\partial \mu} + \frac{1}{1-\mu^2} \frac{\partial^2}{\partial \phi^2} \right] f(\theta, \phi), \quad (\text{C10})$$

which is equivalent to (1) one if we identify $t_{\text{iso}} = 1/\nu_{\text{coll}}$, or, equivalently, $\eta = \omega_g t_{\text{iso}}$.

REFERENCES

- Achterberg, A., & Ball, L. 1994, *A&A*, 285, 687
Achterberg, A., Gallant, Y. A., Kirk, J. G., & Guthmann, A. W. 2001, *MNRAS*, 328, 393
Baring, M. G., Ellison, D. C., & Jones, F. C. 1993, *ApJ*, 409, 327
Bell, A. R. 2014, *Brazilian Journal of Physics*, 44, 415
Bell, A. R., Schure, K. M., & Reville, B. 2011, *MNRAS*, 418, 1208
Bell, A. R., Schure, K. M., Reville, B., & Giacinti, G. 2013, *MNRAS*, 431, 415
Berezhko, E. G., & Völk, H. J. 2000, *A&A*, 357, 283
Biermann, P. L. 1993, *A&A*, 271, 649
Caprioli, D., & Spitkovsky, A. 2014, *ApJ*, 783, 91

- Decker, R. B., & Vlahos, L. 1986, *ApJ*, 306, 710
- Drury, L. O. 1983, *Reports on Progress in Physics*, 46, 973
- . 2011, *MNRAS*, 415, 1807
- Ellison, D. C., Baring, M. G., & Jones, F. C. 1995, *ApJ*, 453, 873
- Ellison, D. C., & Double, G. P. 2004, *Astroparticle Physics*, 22, 323
- Ellison, D. C., & Eichler, D. 1984, *ApJ*, 286, 691
- Ferrand, G., Danos, R. J., Shalchi, A., Safi-Harb, S., Edmon, P., & Mendygral, P. 2014, *ApJ*, 792, 133
- Fisch, N. J., & Kruskal, M. D. 1980, *Journal of Mathematical Physics*, 21, 740
- Gardiner, C. W. 1994, *Handbook of stochastic methods for physics, chemistry and the natural sciences*
- Giacomone, J., & Jokipii, J. R. 1996, *J. Geophys. Res.*, 101, 11095
- Hillas, A. M. 2005, *Journal of Physics G Nuclear Physics*, 31, 95
- Itoh, K. 1944, *Proc. Imp. Acad.*, 20, 519
- Jokipii, J. R. 1971, *Reviews of Geophysics and Space Physics*, 9, 27
- . 1987, *ApJ*, 313, 842
- Jones, F. C., & Ellison, D. C. 1991, *Space Sci. Rev.*, 58, 259
- Kingham, R. J., & Bell, A. R. 2004, *Journal of Computational Physics*, 194, 1
- Kirk, J. G., Guthmann, A. W., Gallant, Y. A., & Achterberg, A. 2000, *ApJ*, 542, 235
- Kirk, J. G., & Heavens, A. F. 1989, *MNRAS*, 239, 995
- Kirk, J. G., & Schneider, P. 1987, *ApJ*, 315, 425
- Lagage, P. O., & Cesarsky, C. J. 1983a, *A&A*, 118, 223
- . 1983b, *A&A*, 125, 249
- le Roux, J. A., Webb, G. M., Shalchi, A., & Zank, G. P. 2010, *ApJ*, 716, 671
- Malkov, M. A., Diamond, P. H., Sagdeev, R. Z., Aharonian, F. A., & Moskalenko, I. V. 2013, *ApJ*, 768, 73
- Matsumoto, Y., Amano, T., & Hoshino, M. 2013, *Physical Review Letters*, 111, 215003
- Matsumoto, Y., Amano, T., Kato, T. N., & Hoshino, M. 2015, *Science*, 347, 974
- Meixner, J., & Schäfer, F. W. 1954, *Mathematische Funktionen und Sphäroidfunktionen*
- Meli, A., & Biermann, P. L. 2006, *A&A*, 454, 687
- Ostrowski, M. 1988, *MNRAS*, 233, 257
- . 1993, *MNRAS*, 264, 248
- Parizot, E., Marcowith, A., Ballet, J., & Gallant, Y. A. 2006, *A&A*, 453, 387
- Parker, E. N. 1958, *ApJ*, 128, 664
- Reville, B., & Bell, A. R. 2012, *MNRAS*, 419, 2433
- Reynolds, S. P., Gaensler, B. M., & Bocchino, F. 2012, *Space Sci. Rev.*, 166, 231
- Reynolds, S. P., & Gilmore, D. M. 1993, *AJ*, 106, 272
- Reynoso, E. M., Hughes, J. P., & Moffett, D. A. 2013, *AJ*, 145, 104
- Schatzman, E. 1963, *Annales d'Astrophysique*, 26, 234
- Shalchi, A. 2009, *Astroparticle Physics*, 31, 237
- Sironi, L., Spitkovsky, A., & Arons, J. 2013, *ApJ*, 771, 54
- Stockem, A., Fiúza, F., Fonseca, R. A., & Silva, L. O. 2012, *ApJ*, 755, 68
- Summerlin, E. J., & Baring, M. G. 2012, *ApJ*, 745, 63
- Takahara, F., & Terasawa, T. 1991, in *Astrophysical Aspects of the Most Energetic Cosmic Rays*, ed. M. Nagano & F. Takahara, 291
- Thompson, I. 2011, *Contemporary Physics*, 52, 497
- Völk, H. J., Berezhko, E. G., & Ksenofontov, L. T. 2005, *A&A*, 433, 229